

Hole pockets in the $t - J$ model

R. Eder and Y. Ohta

Department of Applied Physics, Nagoya University, Nagoya 464-01, Japan

We present an exact diagonalization study of the electron momentum distribution $n(\mathbf{k})$ small clusters of $t - J$ model for different hole concentrations and t/J . Structures in $n(\mathbf{k})$ which were previously interpreted as a ‘large’ Fermi surface are identified as originating from the well known many-body backflow. To obtain reliable information about the true Fermi surface, we focus on the regime $t < J$, where the backflow effect is weak and suppress the formation of a bound state by introducing a density repulsion between holes. We find clear signatures of a Fermi surface which takes the form of small hole pockets. Comparison of the scaling of $n(\mathbf{k})$ and that of the quasiparticle weight with t/J suggests that these pockets persist also for $t > J$.

74.20.-Z, 75.10.Jm, 75.50.Ee

I. INTRODUCTION

The unusual properties of high-temperature superconductors have led to great interest in the physics of correlated electrons near a Mott-Hubbard metal-to-insulator transition. Thereby a particularly intriguing problem is the volume of the Fermi surface (FS) for the slightly less than half-filled band: should one model the doped insulator by a dilute gas of quasiparticles corresponding to the doped holes (this would imply that the volume of the FS is proportional to the hole concentration) or do all electrons take part in the formation of the Fermi surface, so that its volume is identical to that of free electrons? It is the purpose of this paper to present evidence that for finite clusters of $t - J$ model the first picture is the correct one: the FS as deduced from the momentum distribution takes the form of small hole pockets. The $t - J$ model reads:

$$H = -t \sum_{\langle i,j \rangle, \sigma} (\hat{c}_{i,\sigma}^\dagger \hat{c}_{j,\sigma} + H.c.) + J \sum_{\langle i,j \rangle} [\mathbf{S}_i \cdot \mathbf{S}_j - \frac{n_i n_j}{4}].$$

The \mathbf{S}_i are the electronic spin operators, $\hat{c}_{i,\sigma}^\dagger = -c_{i,\sigma}^\dagger (1 - n_{i,-\sigma})$ and the sum over $\langle i, j \rangle$ stands for a summation over all pairs of nearest neighbors. Various authors [1–3] have computed the momentum distribution $n_\sigma(\mathbf{k}) = \langle \hat{c}_{\mathbf{k},\sigma}^\dagger \hat{c}_{\mathbf{k},\sigma} \rangle$ for the two-hole ground state of small clusters of this model (corresponding to a nominal hole concentration of $\sim 10\%$) and found it roughly consistent with a free-electron picture: $n(\mathbf{k})$ is maximum at $\mathbf{k} = (0, 0)$, minimum at $\mathbf{k} = (\pi, \pi)$. It has become customary [2] to cite this as evidence that already at such fairly low hole concentrations the $t - J$ model has a free electron-like (‘large’) FS. It is straightforward to see, however, that this shape of $n(\mathbf{k})$ is simply the consequence of elementary sum-rules and has no significance

for the actual topology of the FS [4]. We have therefore performed a systematic study of the $n(\mathbf{k})$ for various doping levels and t/J .

II. SINGLE HOLE CASE

As compared to the uniform value of $1/2$ for the half-filled case, the introduction of only a single hole changes $n(\vec{k})$ in a rather complex way. Fig. 1 shows $n(\mathbf{k})$ for the single hole-ground states with momentum $\mathbf{k}_0 = (\pi/2, \pi/2)$ in the 16-site cluster and momentum $\mathbf{k}_0 = (2\pi/3, 0)$ in the 18-site cluster. The \mathbf{k} dependence of $n(\mathbf{k})$ is roughly consistent with free electrons, i.e. $n(\mathbf{k})$ is large near $(0, 0)$ and small near (π, π) . This structure, which simply ensures negative kinetic energy [4], is less pronounced the smaller t/J . The second characteristic feature are ‘dips’ at \mathbf{k}_0 for the minority spin (i.e. the ‘hole spin’) and at $\mathbf{k}_0 + (\pi, \pi)$, for both spin directions. These dips are more pronounced for smaller t/J . The question arises which of these features should be associated with the FS, i.e. do we have a ‘large’ FS already for a single hole or is there a ‘hole pocket’ at \mathbf{k}_0 ? We note that the magnitude of the discontinuity in $n(\mathbf{k})$ has to be equal to the weight of the quasiparticle peak in the single particle spectral function, Z_h . Since Z_h has a pronounced [6] (and therefore characteristic) dependence on t/J , a potential FS discontinuity must have the same characteristic dependence on t/J . Then, the ‘depth’ of the dip at \mathbf{k}_0 can be estimated by comparing with a symmetry equivalent \mathbf{k} -point i.e. for $\vec{k}_0 = (\pi/2, \pi/2)$ we consider $\Delta_{dip} = n_\downarrow(-\pi/2, \pi/2) - n_\downarrow(\pi/2, \pi/2)$, for $\vec{k}_0 = (2\pi/3, 0)$ we study $\Delta_{dip} = n_\downarrow(0, 2\pi/3) - n_\downarrow(2\pi/3, 0)$. In Fig. 2 these differences are compared to Z_h (obtained from the single particle spectral function for momentum transfer \mathbf{k}_0 at half-filling) for various values of t/J . Obviously, $\Delta_{dip} = Z_h$ over the entire range of t/J , so that that the dip clearly originates from the Fermi level crossing of the

quasiparticle band, i.e. we have a ‘hole pocket’ at \mathbf{k}_0 . On the other hand, differences $\Delta n(\mathbf{k})$ across the ‘large’ FS always show the opposite behaviour under a variation of t/J as Z_h , indicating that these drops in $n(\mathbf{k})$ are unrelated to any FS crossing. This suggests to associate this structure in $n(\mathbf{k})$ with the well-known ‘backflow’ for interacting Fermi systems [5]. Such a strong backflow effect is by no means surprising if we consider the change in the single particle Greens function upon removing one electron with momentum \mathbf{k}_0 near the FS: naively one might expect that the only effect be the shift of the quasiparticle peak at \mathbf{k}_0 from the photoemission to the inverse photoemission spectrum. If this were true, however, the integrated photoemission weight (which equals the total number of electrons) had decreased only by $Z_h \ll 1$. Hence the bulk of spectral weight shift from photoemission to inverse photoemission must occur for momenta $\mathbf{k} \neq \mathbf{k}_0$, i.e. the strong backflow. What is remarkable is the wide spread of the backflow in \mathbf{k} -space. This implies that for each individual \mathbf{k} the change of $n(\mathbf{k})$ due to removal of an electron at \mathbf{k}_F is $\sim 1/N$, with N the system size. For a small finite hole concentration δ it seems reasonable that the backflow contributions from the individual holes are additive, so that the total backflow contribution would scale with δ .

What remains to be explained are the ‘satellite dips’ at $\mathbf{k}_0 + (\pi, \pi)$. The most natural explanation are antiferromagnetic spin correlations. To see this, let us consider the case $t \ll J$, where the state $1/\sqrt{2}\hat{c}_{\mathbf{k}_0,\downarrow}|\Phi_0\rangle$ (with $|\Phi_0\rangle$ the half-filled ground state) to good approximation is an eigenstate. For this state

$$\begin{aligned} \langle n_{\mathbf{k},\downarrow} \rangle &= \frac{1}{2}(1 - \delta_{\vec{k},\vec{k}_0}) - \frac{2}{3}S(\mathbf{k} - \mathbf{k}_0), \\ \langle n_{\mathbf{k},\uparrow} \rangle &= \frac{1}{2} - \frac{4}{3}S(\mathbf{k} - \mathbf{k}_0) + \frac{1}{N}, \end{aligned} \quad (1)$$

with $S(\mathbf{q})$ the static spin structure factor of $|\Phi_0\rangle$. Since the latter is peaked sharply at $\mathbf{q} = (\pi, \pi)$ we have a natural explanation for the ‘satellite dips’, and it seems reasonable to adopt this explanation also for larger values of t/J .

Summarizing the results obtained so far, we may say that the introduction of a single hole changes $n(\mathbf{k})$ in a rather complex way: there is a dip at the momentum of the hole, which originates from the Fermi level crossing of the quasiparticle band and thus represents the ‘Fermi surface’. The dip is superimposed over a smooth free-electron-like variation, the familiar many-body backflow. As a consequence of the small quasiparticle weight, this backflow is very pronounced in the $t-J$ model. For later reference we note that the backflow contribution to $n(\mathbf{k})$ to good approximation is a function of $|k_x| + |k_y|$ only (this is also confirmed by investigating $n(\mathbf{k})$ for other \mathbf{k}_0). Finally, the strong antiferromagnetic spin correlations produce dips also at $\vec{k}_0 + \vec{Q}$.

This shape of $n(\mathbf{k})$ can be easily understood by recalling [7] that the elementary excitations near the Fermi energy are spin bags, where the hole is dressed by anti-

ferromagnetic spin fluctuations; a simple calculation in terms of the string picture [8] reproduces the numerical results quantitatively.

III. TWO HOLE CASE

We proceed to the ground state with two holes. Various authors [1–3] have found that the free electron-like variation of $n(\mathbf{k})$ observed already for a single hole becomes more pronounced for this doping level, and based on the criterion $n(\mathbf{k}) > 1/2$ [2] the ‘Luttinger Fermi surfaces’ in Fig. 3 would be assigned. However, by the same arguments as for a single hole, these Luttinger Fermi surface are ruled out: Fig. 4 compares the t/J dependence of differences $\Delta n(\mathbf{k})$ across the respective Luttinger FS to that of the quasiparticle weight in the spectral function for the two-hole ground state. Z_h decreases sharply, the $\Delta n(\mathbf{k})$ increase monotonically with t/J . The drop in $n(\mathbf{k})$ upon crossing the large FS thus is obviously unrelated to any true Fermi level crossing. Instead, comparison with Fig. 2 shows that the t/J dependence of the $\Delta n(\mathbf{k})$ is very similar to the backflow contribution for a single hole. More precisely, if we assume that the backflow for the two holes is simply additive, we expect for the ‘large FS’ differences in the two-hole ground state:

$$\Delta n(\mathbf{k}) = \Delta n_{\uparrow}^{(1h)}(\mathbf{k}) + \Delta n_{\downarrow}^{(1h)}(\mathbf{k}), \quad (2)$$

where $\Delta n_{\sigma}^{(1h)}(\mathbf{k})$ are the corresponding differences in the single hole ground state. Fig. 5 compares the ‘large FS’ $\Delta n(\mathbf{k})$ with the estimates obtained from (2) by using the $\Delta n_{\sigma}^{(1h)}(\mathbf{k})$ shown in Fig. 2. Both the magnitude and the t/J scaling are predicted very well by (2), which clearly suggests to associate the ‘large FS’ with the backflow contribution.

The question then is: what is the true FS and how can we make it visible in $n(\mathbf{k})$? Fig. 1 shows that for a single hole the true Fermi surface (i.e. the hole pocket) is most clearly visible for large J/t . This is simply related to the fact that the quasiparticle weight is large in this parameter region (see Fig. 2). Since the t/J -scaling of Z_h is essentially the same at half-filling and in the two hole ground state, (see Figs. 2 and 4) we thus may expect to see the clearest FS signatures for large J/t also in the two-hole ground state.

For more than one hole, however, we face an additional problem: the strong interaction between the holes, which manifests itself e.g. in a sizeable negative binding energy [9,10]. An interacting state of two ‘quasiparticles’ reads

$$|\Psi_0\rangle = \sum_{\mathbf{k}} \Delta(\mathbf{k}) a_{\mathbf{k},\uparrow}^{\dagger} a_{-\mathbf{k},\downarrow}^{\dagger} |vac\rangle. \quad (3)$$

Thus, whereas for a single hole we could fix the location of the pocket simply by choosing the total momentum, in the two-hole ground state the holes will be distributed over different momenta with probability $\sim |\Delta(\mathbf{k})|^2$ and

one may not hope to observe any FS signature unless $\Delta(\mathbf{k})$ is well localized in \mathbf{k} -space, i.e. $\Delta(\mathbf{k}) \sim \delta_{\mathbf{k},\mathbf{k}_0}$ with the quasiparticle ground state \mathbf{k}_0 . This in turn necessitates that the interaction energy be smaller than differences in single particle energy between neighboring \mathbf{k} -points, i.e. weak interaction and sufficiently strong dispersion. With this in mind we add a density interaction term $H_V = V \sum_{\langle i,j \rangle} n_i n_j$, to the Hamiltonian; adjusting the parameter V , one may hope to reach a situation, where H_V to a certain degree ‘cancels’ the intrinsic attractive interaction of the holes. In addition, we include a small next-nearest neighbor hopping term in the Hamiltonian, so as to lift the unfavourable (near) degeneracy of the quasiparticle dispersion along the surface of the magnetic Brillouin zone; we fix the value of the respective hopping integral to be $t' = -0.1t$. For the 16-site cluster this term has the additional advantage that it breaks the spurious additional symmetry due to the mapping to a 2^4 hypercube and selects a unique two-hole groundstate with momentum $(0, 0)$.

Let us stress the following: due to the addition of these terms we are strictly speaking no longer considering the original t - J model. It seems quite plausible, however, that if a FS exists at all, its volume should be changed neither by changing the kinetic energy (t' -term) nor by introducing an additional interaction (V -term).

To demonstrate the adjustment of V , Fig. 6 shows the variation of the hole density correlation function $g(\mathbf{R}) = (1/2) \sum_i \langle (1 - n_{\mathbf{R}_i})(1 - n_{\mathbf{R}_i + \mathbf{R}}) \rangle$ in the two-hole ground states of the 16 and 20 site cluster with V (due to a subtle but understandable pathology in its geometry, analogous results cannot be obtained for the 18-site cluster, see Appendix). Its essentially identical behaviour in both clusters clearly signals a change of the net interaction between the holes from attraction to repulsion. For intermediate values of V , on the other hand, $g(\mathbf{R})$ is quite homogeneous indicating that the single particle delocalization energy of the holes dominates over their interaction. Given this plus the large Z_h we should therefore be in an optimal position for observing the FS.

Figs. 7 and 8 show the single particle spectral function $A(\mathbf{k}, \omega)$ for $J/t=2$ and the momentum distribution for $J/t=1$ and $J/t=2$ (and the respective ‘optimal’ V). In the spectral function, the chemical potential E_F is located near the top but within a group of pronounced peaks, well separated from another such group in the inverse photoemission spectrum. There are pronounced peaks both immediately above and below E_F which comprise the bulk of spectral weight for the respective momenta. Corresponding to the well defined ‘quasiparticle peaks’ in the spectral function, $n(\mathbf{k})$ exhibits a sharp variation: hole pockets at $(\pi, 0)$ and $(0, \pi)$. They are superimposed over the familiar backflow contribution, which again has the generic free electron like form so as to ensure negative kinetic energy. Fig. 8 also gives the values of the quasiparticle weight for the ‘Fermi momenta’. For $(2\pi/5, 3\pi/5)$ in the 20-site cluster the ‘quasiparticle peak’ in the photoemission spectrum (PES) actually

consists of two peaks with approximately equal weight; we consider these as a single ‘broadened’ peak, so that the two weights should be added. This is supported by the good agreement with Z_h at $(\pi/2, \pi/2)$ in the 16-site cluster (where no splitting occurs) and the reasonable agreement with the Z_h deduced from the inverse photoemission spectrum (IPES) at $(\pi, 0)$ (where no splitting occurs either). The ‘depth’ of the pockets approximately equals Z_h and both quantities consistently decrease with decreasing J/t .

A somewhat astonishing feature of these results is the location of the pockets at $(\pi, 0)$ rather than at $(\pi/2, \pi/2)$. This can be traced back to the point group symmetry of the ground two-hole ground state: when the symmetry of the half-filled ground state is A_1 (or s), that of the two-hole ground state is B_1 (or $d_{x^2-y^2}$) and vice versa (the former situation is realized in the 16 and 18-site cluster, the latter in the 20-site cluster). Addition of two holes thus always is equivalent to adding an object with $d_{x^2-y^2}$ -symmetry, which implies that the pair wave function $\Delta(\mathbf{k})$ in (3) should have this symmetry as well. This in turn implies $\Delta(\mathbf{k}) = 0$ for \mathbf{k} along $(1, 1)$, so that occupation of $(\pi, 0)$ is favoured.

Fig. 9 shows the ‘FS discontinuities’ in the 4×4 cluster under a variation of the repulsion strength V . They show maxima when the density correlation function is most homogeneous, precisely as one would expect for Fermions with a variable interaction strength. In the spectral function the reduction of the discontinuities as $V \rightarrow 0$ manifests itself by the reduction in intensity of the big IPES peak at $(\pi, 0)$ and the appearance of small low energy IPES peaks at the momenta next to $(\pi, 0)$: the pockets are ‘washed out’. We note that the $\Delta n(\mathbf{k})$ across the ‘large’ FS remains unaffected, another indication that it is unrelated to low-energy physics.

A possible explanation for the hole pocket FS would be spin-density-wave-type broken symmetry: although the ground states under consideration are spin singlets, this might be realized if the fluctuations of the staggered magnetization M_S were slow as compared to the hole motion, so that the holes move under the influence of an ‘adiabatically varying’ staggered field. A possible criterion for this situation would be $\tau_{tr} \omega_{AF} \ll 2\pi$, where τ_{tr} is the time it takes for a hole to transverse the cluster and ω_{AF} is the frequency of fluctuations of M_S . We estimate (for $J/t = 2$) the group velocity of the holes from the dispersion of the ‘quasiparticle peak’ in the PES spectrum and, using the energies indicated by arrows in Fig. 7 for the 20-site cluster and the peaks at $(\pi/2, 0)$ and $(\pi/2, \pi/2)$ for the 16-site cluster, we find $\tau_{tr} \simeq 2\pi/0.5t(2\pi/0.2t)$ for the 20 (16)-site cluster. Typical frequencies for fluctuations of M_S can be obtained from its correlation function, which, up to a constant, equals the dynamical spin susceptibility for momentum transfer (π, π) ; a rigorous lower bound on ω_{AF} thus can be obtained by subtracting the ground state energy from the energy of the lowest state with total momentum (π, π) and the same point group symmetry as the ground state.

This gives $\omega_{AF} > 0.9t(1.2t)$ for the 20 (16) cluster, i.e. $\tau_{tr} \cdot \omega_{AF} > 2\pi$. ‘Almost static’ Néel order thus can be ruled out as origin of the small FS, even for this fairly large value of J/t .

As an additional check we have introduced exchange terms J' between 2^{nd} and 3^{rd} nearest neighbors to reduce the spin correlations and again optimized the repulsion to enable ‘free’ hole motion. Ground state properties of this (highly artificial) model are summarized in Fig. 10: the momentum distribution, hole density correlation function and spin correlation function $S(|\mathbf{R}|) = \exp(i\mathbf{Q} \cdot \mathbf{R}) \langle \mathbf{S}_i \cdot \mathbf{S}_{i+\mathbf{R}} \rangle$ (with $\mathbf{Q} = (\pi, \pi)$). The density correlation function is homogeneous (no charge ordering), the spin correlations decay rapidly (no long range antiferromagnetic or spiral ordering) but still there are unambiguous hole pockets in $n(\mathbf{k})$. The only possible conclusion is that it is only the large Z_h which makes the pockets visible in the large J region, and not the onset of any kind of ordering.

While the hole pockets can be made clearly visible for large J , the situation is more involved for $t > J$. In this parameter region the small overlap between ‘quasiparticle’ and ‘bare hole’ (as manifested by the small Z_h) makes the V -term (which couples only to the bare hole) increasingly inefficient in enforcing a noninteracting state: rather than separating from each other, the two holes remain bound on second-nearest neighbors up to fairly large values of V and the ‘crossover’ from attraction to repulsion, which gave an unambiguous prescription for choosing V , cannot be obtained any more. We thus abandon both the V and t' terms and adopt a more indirect way of reasoning.

In the single hole case, we found that the pocket was superimposed over the smooth backflow contribution. We assume that the situation for 2 holes is similar, only with the additional complication that the pockets are now ‘washed out’ due to the interaction between holes (see Fig. 9). Therefore we expect that $n(\mathbf{k})$ can be written as

$$n(\mathbf{k}) = n_{back}(\mathbf{k}) + Z_h \cdot |\Delta(\mathbf{k})|^2, \quad (4)$$

with the pair wave function $\Delta(\mathbf{k})$ introduced in (3). As discussed above, the point group symmetry of the two-hole ground state necessitates that $\Delta(\mathbf{k})$ has $d_{x^2-y^2}$ symmetry, so that the pockets are located at $(\pi, 0)$. Then, since the symmetry of the ground state is unchanged by adding either the t' or V term, we conclude that this should also hold true in the absence of these terms.

Since $n_{back}(\mathbf{k})$ to good approximation is a function of $|k_x| + |k_y|$ only (see Fig. 1), this contribution can be eliminated by forming the difference of two momenta with (almost) equal $|k_x| + |k_y|$. Next, if we choose one of these momenta along (or near) the $(1, 1)$ direction, where the $d_{x^2-y^2}$ -symmetry requires that $\Delta(\mathbf{k})$ vanishes (or is small), and the other at (or near) $(\pi, 0)$ we should obtain

$$\Delta n(\mathbf{k}) = Z_h \cdot |\Delta(\pi, 0)|^2, \quad (5)$$

so that, in contrast to the ‘large FS’ differences indicated in Fig. 3 this difference should scale with Z_h . To check this prediction, the t/J dependence of various such differences is shown in Fig. 11 and obviously, they are to excellent approximation proportional to Z_h over a wide range of t/J . The scaling of $n(\mathbf{k})$ with t/J thus is completely consistent with the assumptions

- a) that there are washed out hole pockets at $(\pi, 0)$,
- b) that these are superimposed over the smooth backflow contribution, which is the sum of the backflows for the two individual holes (see Fig. 5).

IV. COMPARISON WITH OTHER NUMERICAL STUDIES AND EXPERIMENT

While the hole pockets are very clearly visible for large J , the evidence for their existence in the physical regime is of a more indirect character. A comparison with other numerical calculations and experiments on high-temperature superconductors is therefore necessary. As far as numerical studies on small clusters are concerned, hole pockets and/or rigid band behaviour upon doping are consistently suggested by most of the available numerical calculations. For the $t - J$ model, Poilblanc and Dagotto [11] studied the $A(\mathbf{k}, \omega)$ for single hole states and concluded that the two-hole ground state in the 4×4 cluster shows hole pockets at $(\pi, 0)$, in agreement with the present result. On the other hand, Stephan and Horsch [2] studied $n(\mathbf{k})$ and $A(\mathbf{k}, \omega)$ for the two-hole ground state and concluded that there is neither rigid band behaviour nor hole pockets. However, these authors based their conclusions solely on the qualitative inspection of a rather limited data set, which is largely irrelevant [4] for deciding the FS topology. In addition to the inconsistent scaling behaviour found above (Fig. 4), numerical calculation of $A(\mathbf{k}, \omega)$ for the 20-site cluster [14] rules out the Luttinger FS postulated by Stephan and Horsch.

Castillo and Balseiro [12] computed the Hall constant and found its sign near half-filling to be consistent with a hole-like FS, i.e. with hole pockets. Gooding *et al.* [13] studied the doping dependence of the spin correlation function in clusters with special geometry and also found indications of rigid-band behaviour. Finally, a systematic study of the doping dependence of the single particle spectral function [14] shows rigid-band behaviour, i.e. holes are filled into the quasiparticle band present at half-filling (which naturally implies hole pockets).

The situation is quite similar for the Hubbard model. While the generic [4] free-electron like shape of $n(\mathbf{k})$ found in earlier Monte-Carlo studies [15] was initially considered as evidence against hole pockets, more careful and systematic analysis [16] showed that hole pockets are in fact remarkably consistent with the numerical data, their nonobservation in the earlier studies being simply the consequence of thermal smearing. It seems fair to say that the available numerical results for small clusters of both Hubbard and $t - J$ models, when interpreted with

care, are all consistent with rigid band behaviour and/or hole pockets.

Let us next discuss experimental results on high-temperature superconductors assuming that the hole pockets found in the cluster studies persist in the real systems. The volume of the FS associated with the $Cu - O$ plane-derived bands in these materials presents a well-known puzzle: early photoemission experiments [18] show bands, which disperse towards the Fermi energy and vanish at points in \vec{k} -space which are roughly located on the free electron FS corresponding to electron density $1 - \delta$, where δ is the hole concentration; on the other hand transport properties can be modelled well [19,20] by assuming a FS with a volume $\sim \delta$. In a Fermi liquid, the apparently contradicting quantities actually fall into distinct classes: photoemission spectra depend on Z_h , transport properties do not. Hence, if one wants to resolve the discrepancy entirely within a Fermi liquid-like picture, the simplest way would be to assume a ‘small’ FS and explain the photoemission results by a systematic variation of Z_h along the band which forms the FS, similar to the ‘shadow band’ picture [21]. A trivial argument for such a strong \mathbf{k} -dependence of the quasiparticle weight is, that a distribution of PES weight in the Brillouin zone (and hence a $n(\mathbf{k})$) that resembles the noninteracting FS, always optimizes the expectation value of the kinetic energy. Therefore it is favourable if those parts of the band structure, which lie inside the free-electron FS have large spectral weight, and the parts outside small weight. Then, it seems that in a recent photoemission study by Aebi *et al.* [22], structures which are very consistent with such a shadow band scenario have indeed been observed. Moreover, another key feature of the dispersion relation for a single hole, namely the extended flat region near $(\pi, 0)$ [23,24] has also been found as an universal feature of high temperature superconductors [25,26] Adopting a rigid band/hole pocket scenario thus would explain many experiments in a very simple and natural way, which moreover is remarkably consistent with the existing numerical data as a whole.

V. CONCLUSION

We have discussed the problems in directly determining the FS from $n(\mathbf{k})$ in the $t-J$ model: small quasiparticle weight, a pronounced ‘backflow’ effect and strong interaction between the doped holes. We have then examined the single particle spectral function and $n(\mathbf{k})$ in a situation where these problems were largely avoided and found signatures of a FS which takes the form of small hole-pockets. Analysis of the scaling of $n(\mathbf{k})$ with t/J suggested that these pockets also persist in the regime $t > J$. Available numerical data all support this picture, and we have outlined a possible scenario to reconcile experiments on high-temperature superconductors. The assumption of a small Fermi surface implies that the phase of some given basis state is determined by a

Slater determinant of rank $N - N_e$, (N_e being the number of electrons) rather than N_e (as it would be e.g. in a Gutzwiller projected Fermi sea). Moreover, it would not be the positions of the electrons which enter this Slater determinant, but those of the hole-like quasiparticles, so that we have a very different nature of long range phase coherence. The Fermi surface in an interacting system, being a ‘remnant’ of the noninteracting one, is obviously a consequence of the requirements to have minimum kinetic energy and to satisfy the Pauli principle. On the other hand, close to half-filling most of the electrons are immobile, so that the gain in kinetic energy from creating the long range phase coherence between electrons (which is responsible for the singularity of $n(\mathbf{k})$) may not be very large. On the other hand, the vacancies are almost unconditionally mobile, so that phase coherence between holes may be more favourable.

It is a pleasure for us to acknowledge numerous instructive discussions with Professor S. Maekawa. Financial support of R. E. by the Japan Society for the Promotion of Science is most gratefully acknowledged. Computations were partly carried out at the computer Center of the Institute for Molecular Science, Okazaki National Research Institutes.

VI. APPENDIX

The 18-site cluster has a pathological geometry, which does not allow for an unbound state of two particles with $d_{x^2-y^2}$ -symmetry. The ultimate reason is that the primitive lattice translations in this cluster are $(3, 3)$ and $(3, -3)$. Writing an interacting two-hole state in real space, we have

$$|\Phi\rangle = \sum_i \sum_{\mathbf{R}} \phi(\mathbf{R}) a_{i,\uparrow}^\dagger a_{i+\mathbf{R},\downarrow}^\dagger |vac\rangle \quad (6)$$

If we choose $\mathbf{R} = (2, 1)$, rotate counterclockwise by $\pi/2$, reflect by the x -axis and add $(3, 3)$ we recover the original vector. A state with $d_{x^2-y^2}$ symmetry picks up a factor of (-1) during these operations, hence $\phi(2, 1) = 0$. Analogous reasoning shows that $\phi(3, 0) = 0$, so that all large distances between particles are ‘symmetry forbidden’ (possible distance in this cluster are $(1, 0)$, $(1, 1)$, $(2, 0)$ $(2, 1)$ and $(3, 0)$). The ‘unbinding transition’ for this cluster thus can occur only via level crossing and this is indeed the case: when V is switched on in the $d_{x^2-y^2}$ ground state, the holes stay close to each other even for fairly large values of V . Instead, at $V \sim 3t$ (for $J/t = 2$) a level crossing occurs, and a new ground state with momentum $(2\pi/3, 0)$ is stabilized.

FIG. 1. Momentum distribution for the single hole ground state with $S_z = 1/2$ (i.e. with a ‘ \downarrow -hole’) of the 4×4 cluster with $t/J = 4$ (top) of the 4×4 cluster with $t/J = 1$ (middle) 18-site cluster with $t/J = 2$ (bottom). The upper values refer to the majority spin, the lower values to the minority spin, the ground state momentum \mathbf{k}_0 is marked by a black box and $\mathbf{k}_0 + (\pi, \pi)$ by a dotted box.

FIG. 2. Comparison of the t/J -dependence of Z_h at half-filling (dark squares) and various differences $\Delta n(\mathbf{k})$ in the single hole ground states with $S_z = 1/2$. Shown is the ‘depth’ of the pockets (light circles) and differences across the ‘large FS’ (up and down triangles).

FIG. 3. Allowed momenta and ‘Luttinger Fermi surfaces’ for various clusters. The ‘Fermi momenta’ are denoted by \mathbf{k}_F .

FIG. 4. Comparison of the t/J -dependence of Z_h (dark squares, obtained from the photoemission spectra at the \mathbf{k}_F indicated in Fig. 3) and the differences $\Delta n(\mathbf{k})$ between pairs of momenta connected by dashed lines in Fig. 3 (light squares and circles).

FIG. 5. Comparison of the t/J -dependence of the $\Delta n(\mathbf{k})$ shown in Fig. 3 (light squares) and the estimates obtained from (2) by using the single hole $\Delta n(\mathbf{k})$ in Fig. 2 (dark squares).

FIG. 6. V -dependence of the hole density correlation function $g(\mathbf{R})$ in the ground state of $t-t'-J-V$ clusters with 2 holes ($J/t=2$).

FIG. 7. Single particle spectral function for the $t-t'-J-V$ model with 2 holes and $J/t=2$ for the 20-site with $V/t=2.5$ (a) as well as the 16-site cluster with $V/t=2.4$ (b). Delta functions have been replaced by Lorentzians of width $0.05t$. The frequency region $\omega < E_F$ ($\omega > E_F$) corresponds to photoemission (inverse photoemission).

FIG. 8. Momentum distribution in the two-hole ground state of the cluster $t-t'-J-V$ models with $J/t=2$ and $V/t=2.5$ ($V/t=2.4$) for the 20-site (16-site) cluster (a) and for $J/t=1$ and $V/t=3.0$ ($V/t=2.0$) for the 20-site (16-site) cluster (b). For the ‘Fermi momenta’ the quasiparticle weight Z_h is given in brackets.

FIG. 9. V dependence of selected $\Delta n(\mathbf{k})$ in the 4×4 cluster, parameters are like in Fig. 6.

FIG. 10. Hole density correlation function $g(\mathbf{R})$ (dark circles), spin correlation function $S(\mathbf{R})$ (light squares) and $n(\mathbf{k})$ (inset) for the ground state with spin frustration. Parameter values are $J = 2$, $J' = 0.75$, $t' = -0.1$. There is a density repulsion of strength $1.7t$ between holes on 1^{st} , 2^{nd} and 3^{rd} nearest neighbors.

FIG. 11. Comparison of the scaling of Z_h (dark squares) and selected difference $\Delta n(\mathbf{k})$ (light squares) with t/J : $1.5 \cdot (n(\pi/2, \pi/2) - n(\pi, 0))$ (16-site), $2.8 \cdot (n(\pi/3, \pi/3) - n(2\pi/3, 0))$ (18-site) and $3.6 \cdot (n(\pi/5, 3\pi/5) - n(\pi, 0))$ (20-site).

-
- [1] J. Bonča, P. Prelovšek, and I. Sega, Solid State Commun. **78**, 109 (1991).
 - [2] W. Stephan and P. Horsch, Phys. Rev. Lett. **66**, 2258 (1990).
 - [3] H.-Q. Ding, Physica C **203**, 91, (1992).
 - [4] R. Eder and Y. Ohta, Phys. Rev. Lett. **72**, 2816 (1994).
 - [5] P. Nozieres, Interacting Fermi systems, W. A. Benjamin, New York 1969.
 - [6] E. Dagotto, R. Joynt, A. Moreo, S. Bacci, and E. Dagliano Phys. Rev. B **41**, 9049 (1990).
 - [7] R. Eder and Y. Ohta, Phys. Rev. B, in press. (also: cond-mat sissa-preprint 9406098).
 - [8] R. Eder und K. W. Becker, Phys. Rev. B **44**, 6982 (1991).
 - [9] J. Bonča, P. Prelovšek, and I. Sega, Phys. Rev. B **39**, 7074 (1989).
 - [10] Y. Hasegawa, D. Poilblanc, Phys. Rev. B **40**, 9035 (1989).
 - [11] D. Poilblanc and E. Dagotto, Phys. Rev. B **42**, 4861 (1990).
 - [12] H. E. Castillo and C. A. Balseiro, Phys. Rev. Lett. **68**, 121 (1992).
 - [13] R. J. Gooding, K. J. E. Vos, and P. W. Leung, Phys. Rev. B **49**, 4119 (1994).
 - [14] R. Eder, Y. Ohta, and T. Shimozato, Phys. Rev. B, in press. (also: cond-mat sissa-preprint 9406064).
 - [15] A. Moreo *et al.*, Phys. Rev. B **41**, 2313 (1990).
 - [16] A. Moreo and D. Duffy, cond-mat sissa-preprint 9407039.
 - [17] A. P. Kampf and J. R. Schrieffer, Phys. Rev. B **42**, 7967 (1990).
 - [18] C. G. Olson *et al.*, Science **245**, 731 (1989).
 - [19] S. A. Trugman, Phys. Rev. Lett. **65**, 500 (1990).
 - [20] E. Dagotto, A. Nazarenko, and M. Bonisegni, preprint
 - [21] A. P. Kampf and J. R. Schrieffer, Phys. Rev. B **42**, 7967 (1990).
 - [22] P. Aebi *et al.*, Phys. Rev. Lett. **72**, 2757 (1993).
 - [23] J. Inoue and S. Maekawa, J. Phys. Soc. Jpn. **59**, 2110 (1990).
 - [24] R. Eder and K. W. Becker, Z. Phys. **78**, 219 (1990).
 - [25] D. S. Dessau *et al.*, Phys. Rev. Lett. **71**, 2781 (1993).
 - [26] A. A. Abrikosov, J. C. Campuzano, and K. Gofron, Phys-

ica C 214, 73 (1993).

Fig. 1

π	0.4378	0.5364	0.4211	0.4026
	0.3823	0.4647	0.4053	0.3796
$\pi/2$	0.5378	0.5558	0.5310	0.4211
	0.4650	0.4946	0.3242	0.4053
0	0.5589	0.5531	0.5558	0.5364
	0.4966	0.4937	0.4946	0.4647
$-\pi/2$	0.4182	0.5589	0.5378	0.4650
	0.3854	0.4966	0.4650	0.3823
	$-\pi/2$	0	$\pi/2$	π

π	0.4521	0.5293	0.4512	0.4084
	0.4142	0.4698	0.4352	0.4030
$\pi/2$	0.5317	0.5601	0.5457	0.4512
	0.4678	0.4968	0.1948	0.4352
0	0.5604	0.5587	0.5601	0.5293
	0.4929	0.4980	0.4968	0.4698
$-\pi/2$	0.3178	0.5604	0.5317	0.4521
	0.3506	0.4929	0.4678	0.4142
	$-\pi/2$	0	$\pi/2$	π

π		0.3663		0.4733		0.4252
		0.3837		0.4587		0.3982
$2\pi/3$	0.4596		0.5484		0.4374	
	0.4038		0.4940		0.4223	
$\pi/3$		0.5535		0.5541		0.4898
		0.4976		0.4985		0.4323
0	0.5485		0.5491		0.5517	
	0.4815		0.4962		0.2847	
$-\pi/3$		0.5535		0.5541		0.4898
		0.4976		0.4985		0.4323
$-2\pi/3$	0.4596		0.5484		0.4374	
	0.4038		0.4940		0.4223	
	$-2\pi/3$	$-\pi/3$	0	$\pi/3$	$2\pi/3$	π

Fig. 2

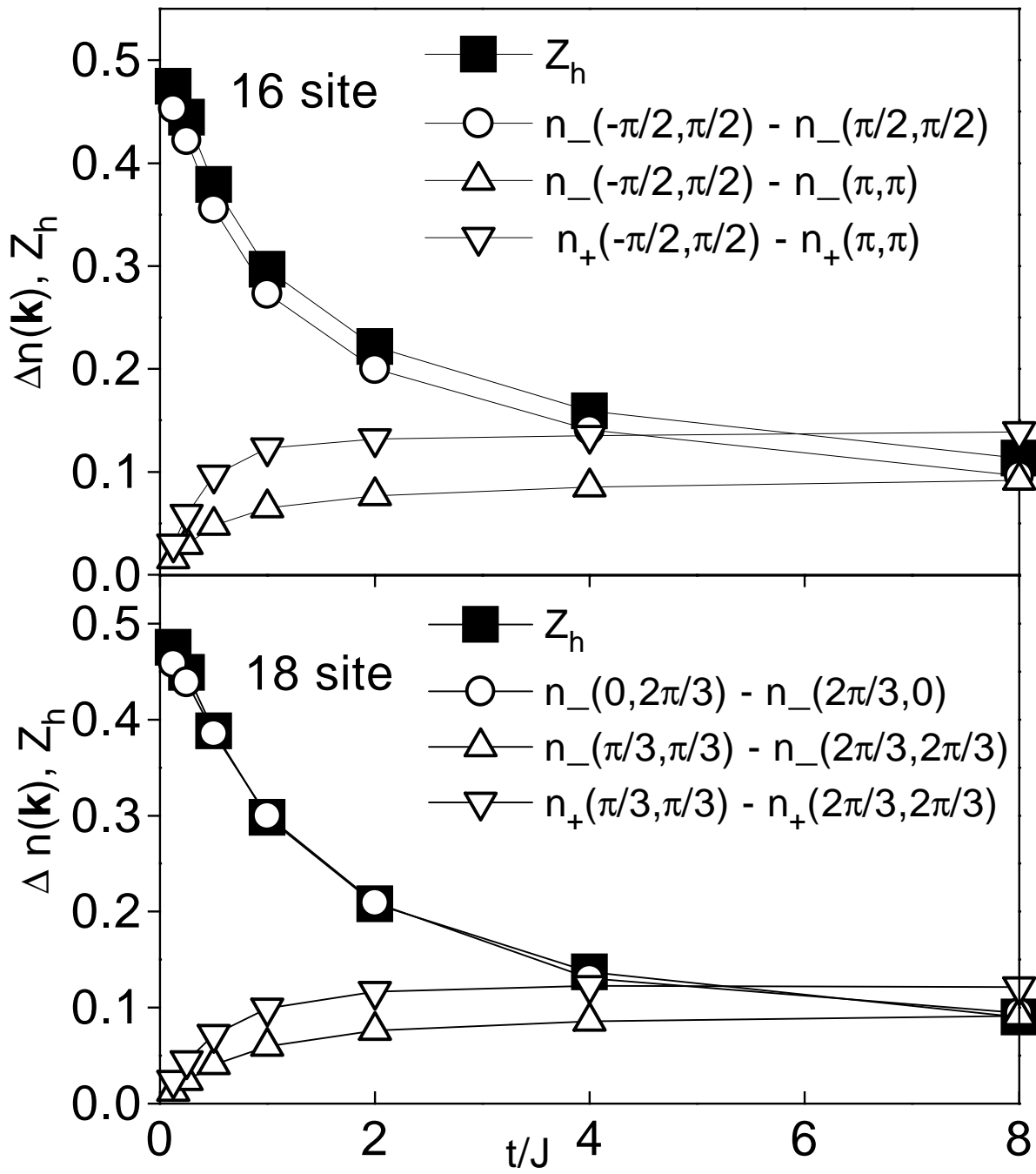


Fig. 3

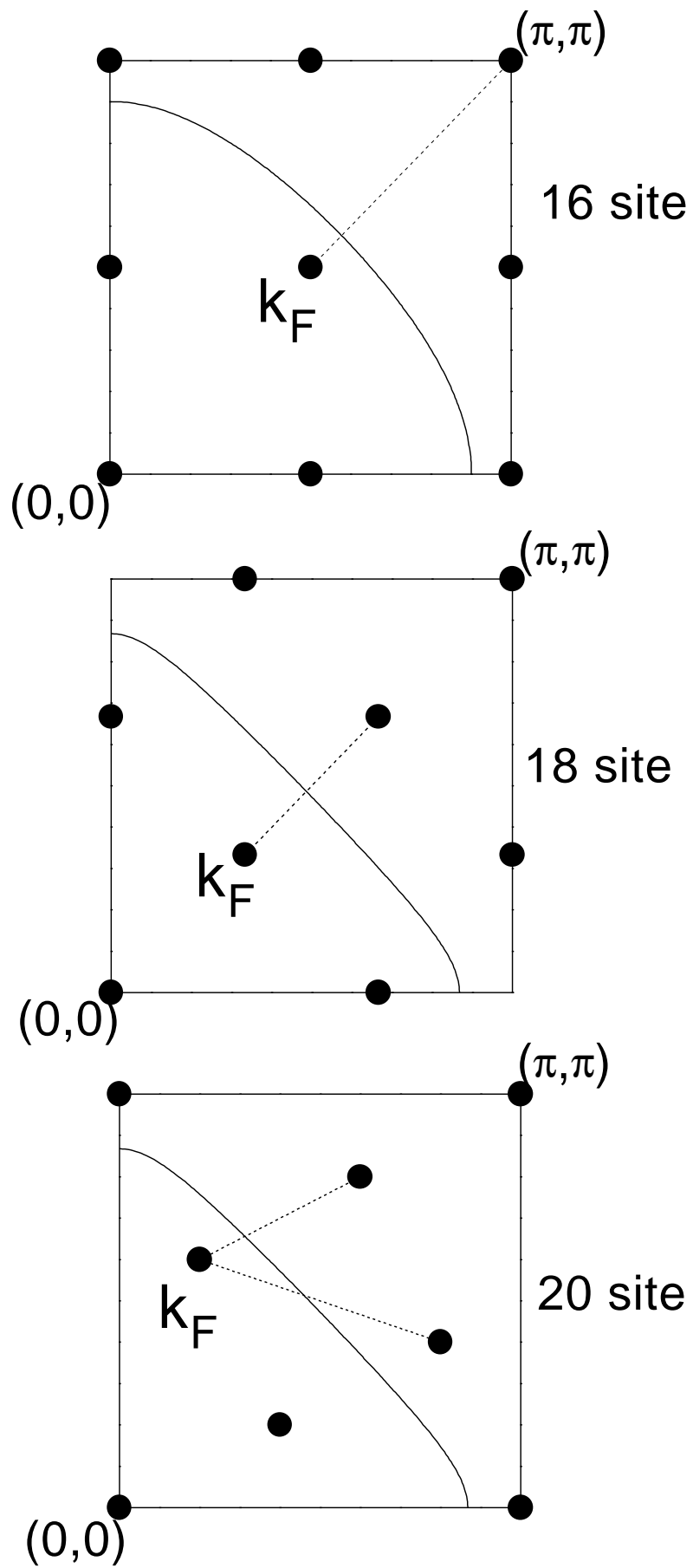


Fig. 4

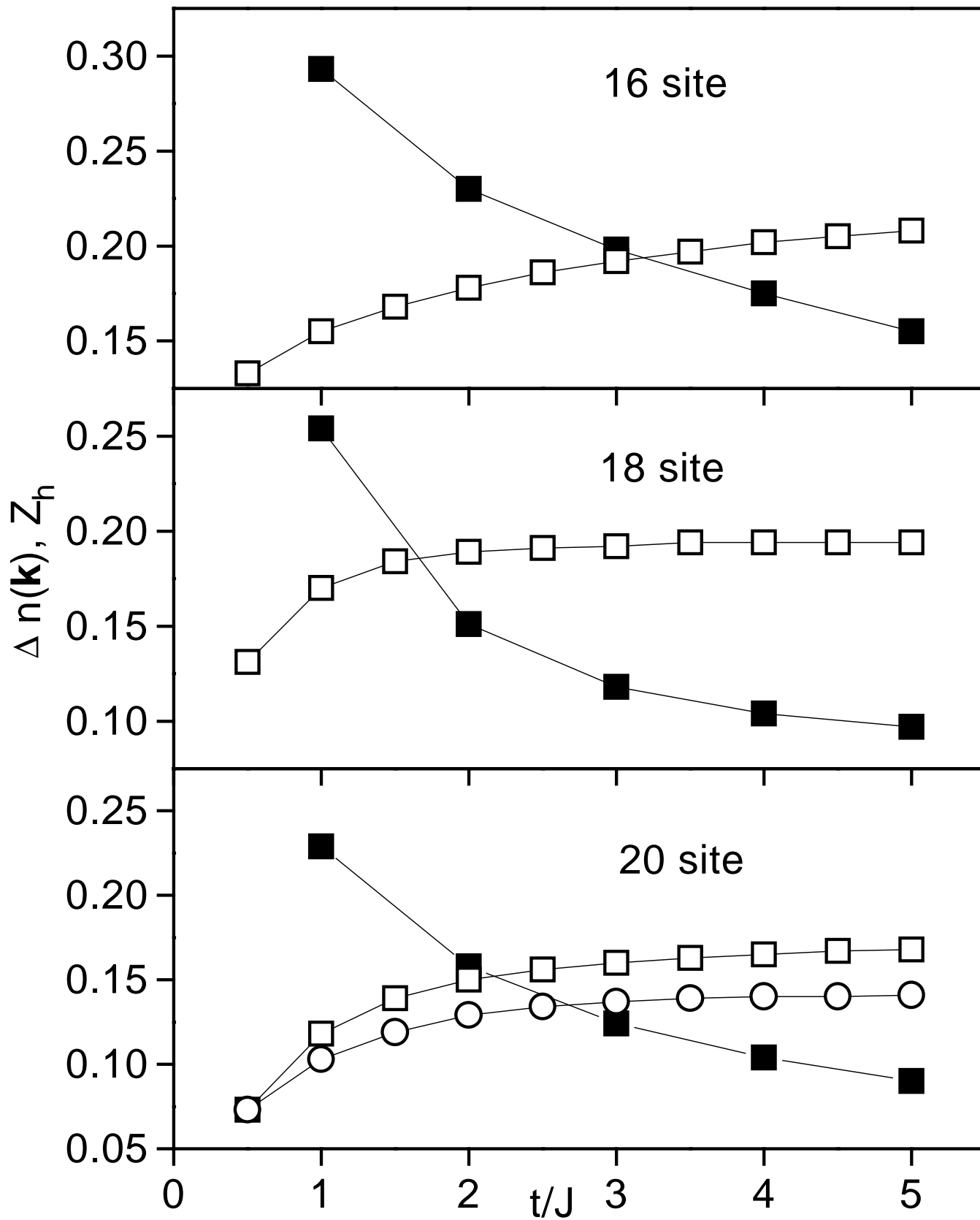


Fig. 6

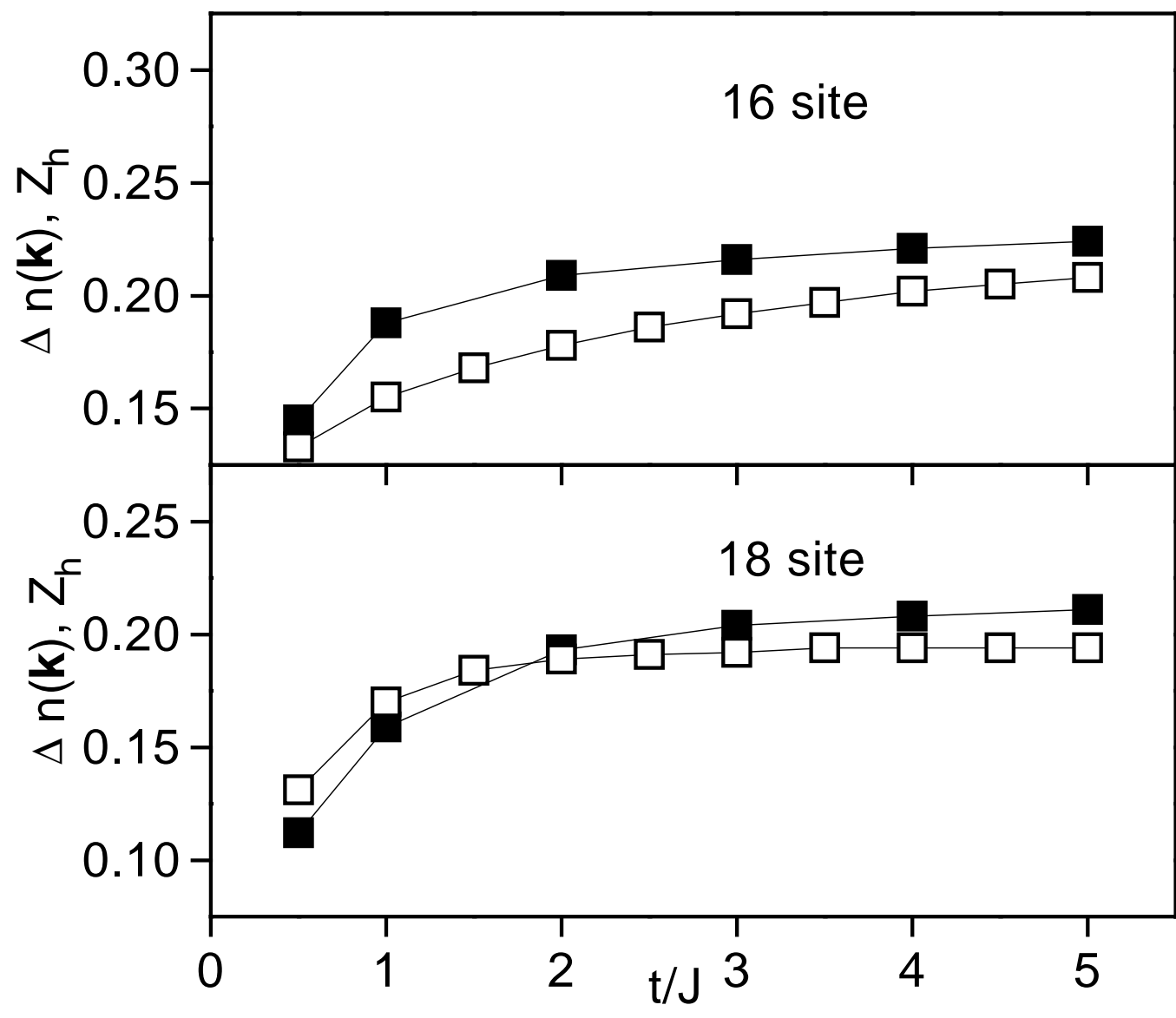
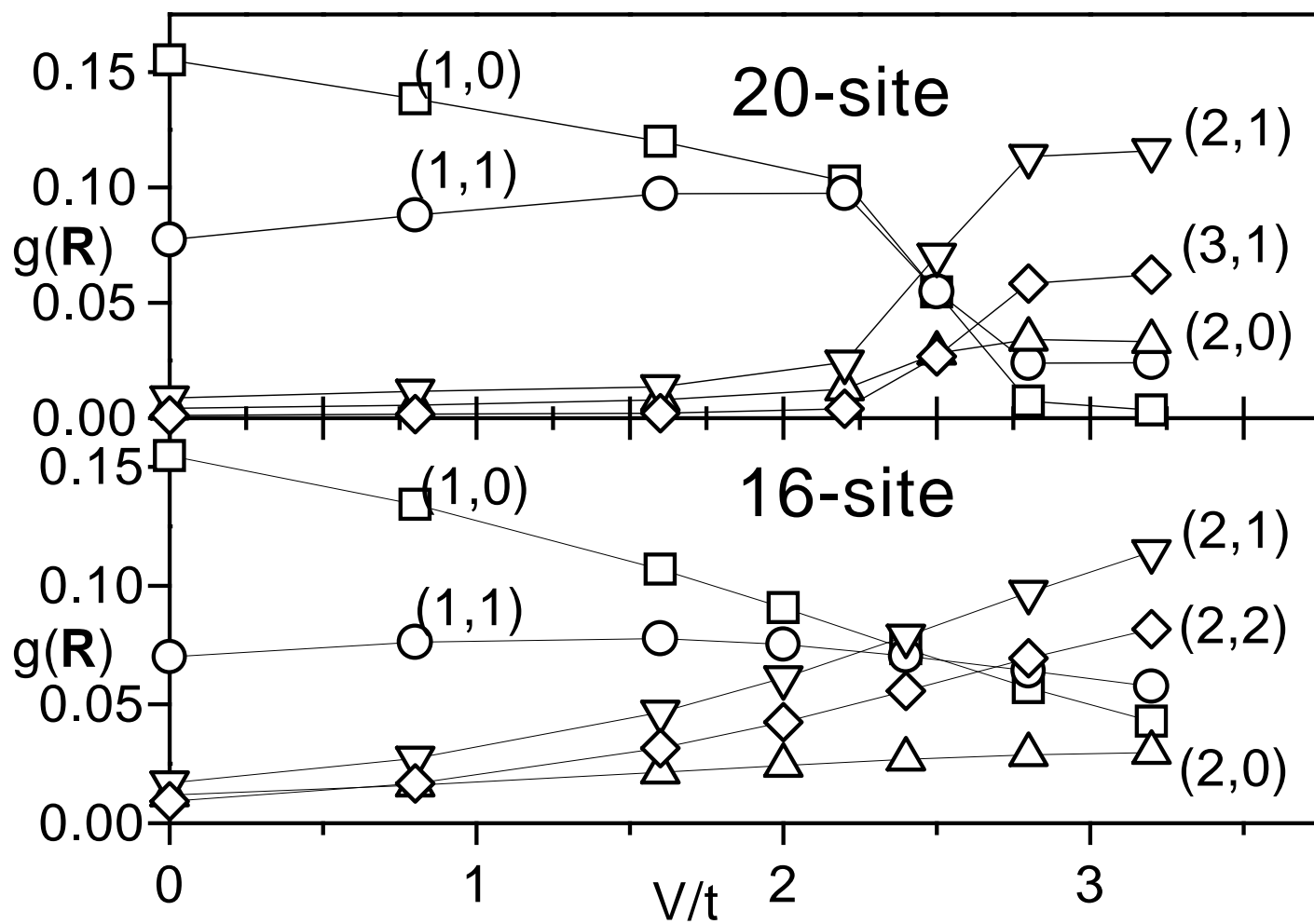


Fig. 6



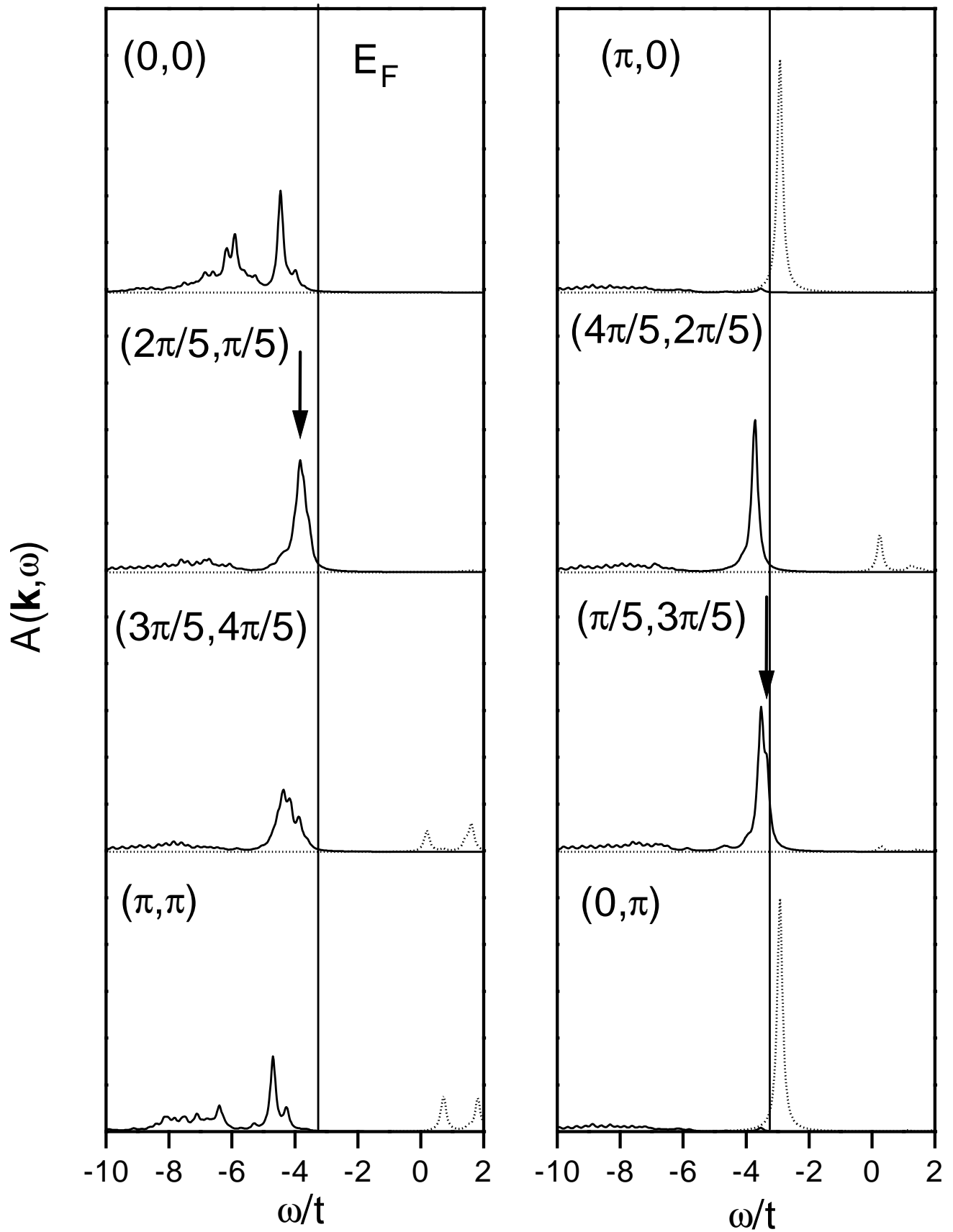


Fig. 7b

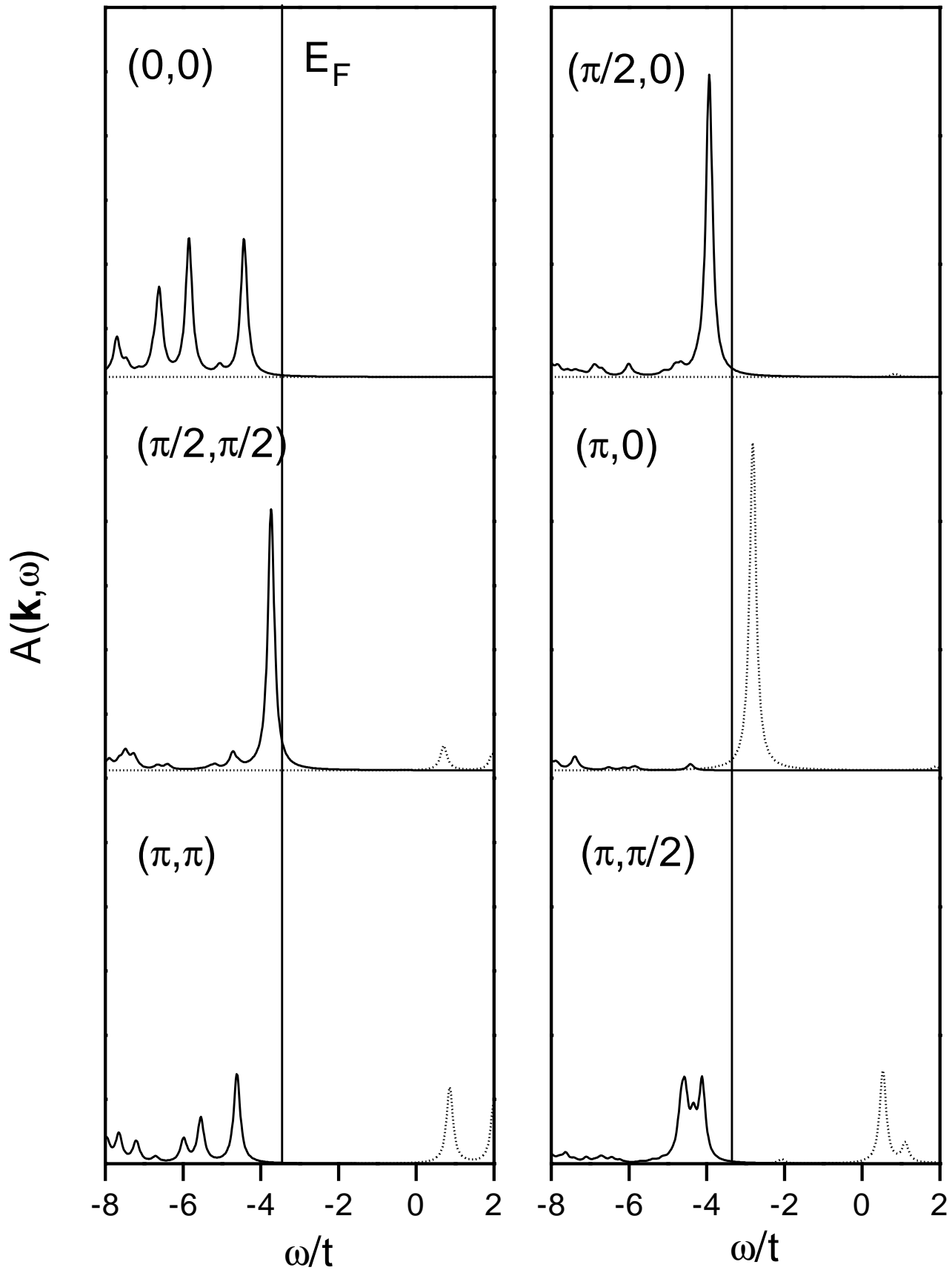
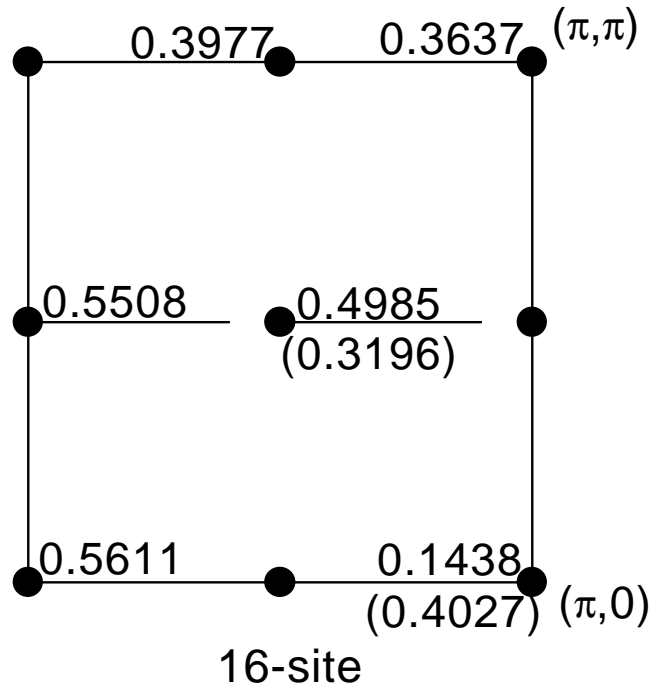
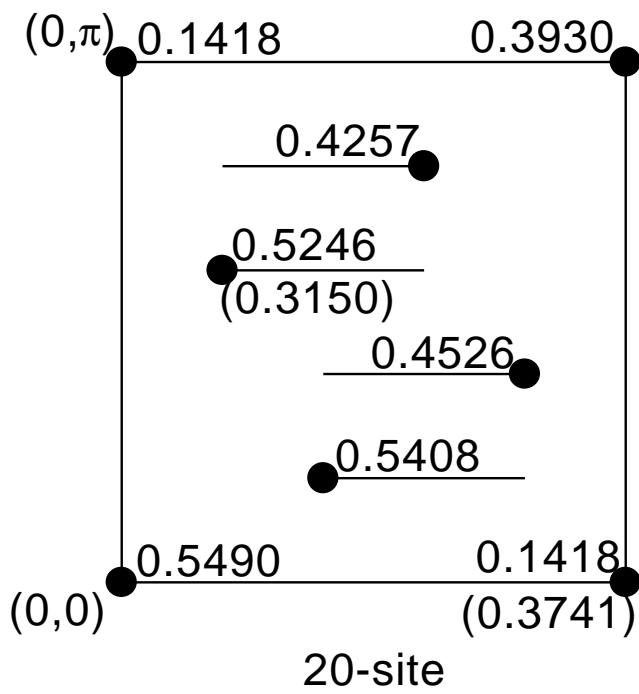


Fig. 8a



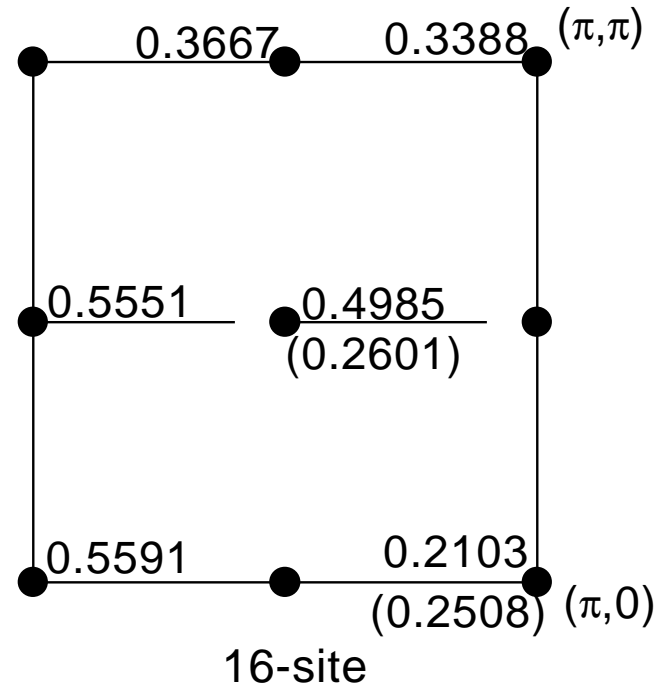
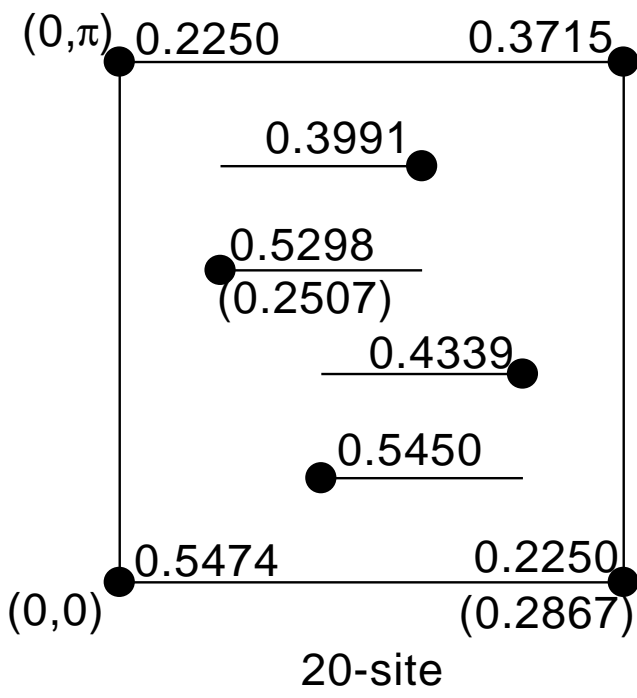


Fig. 9

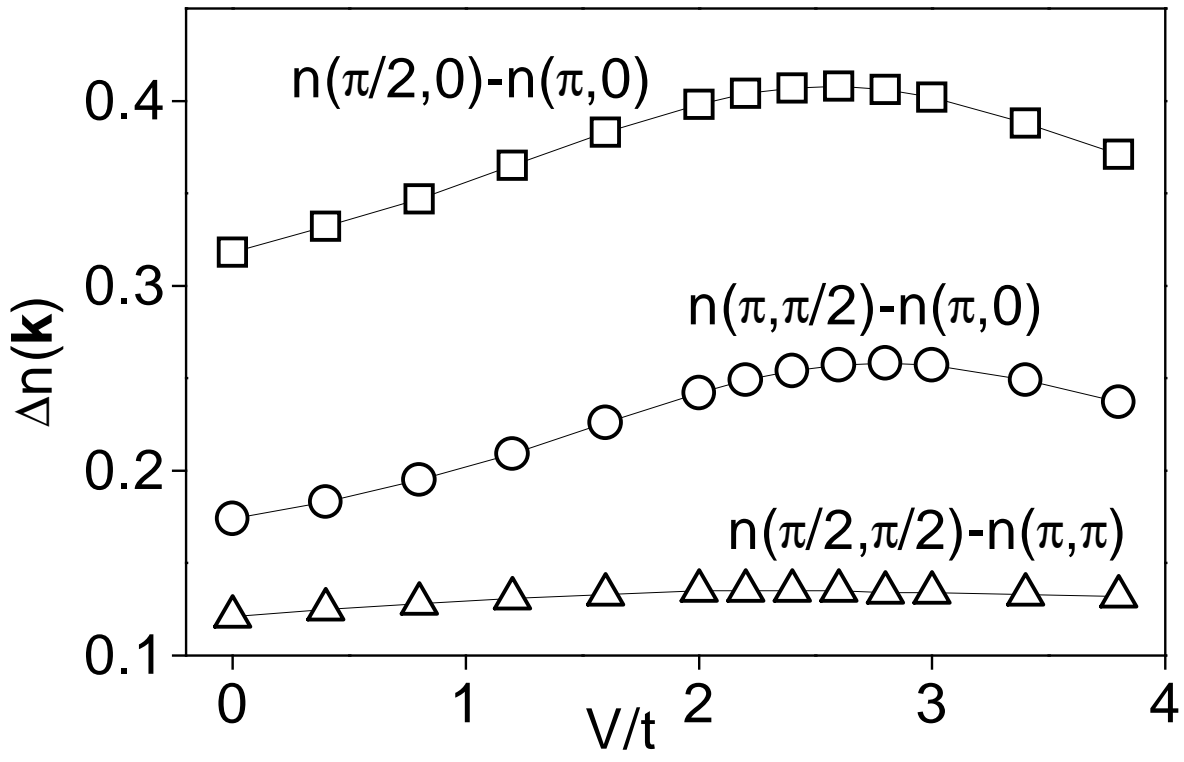


Fig. 10

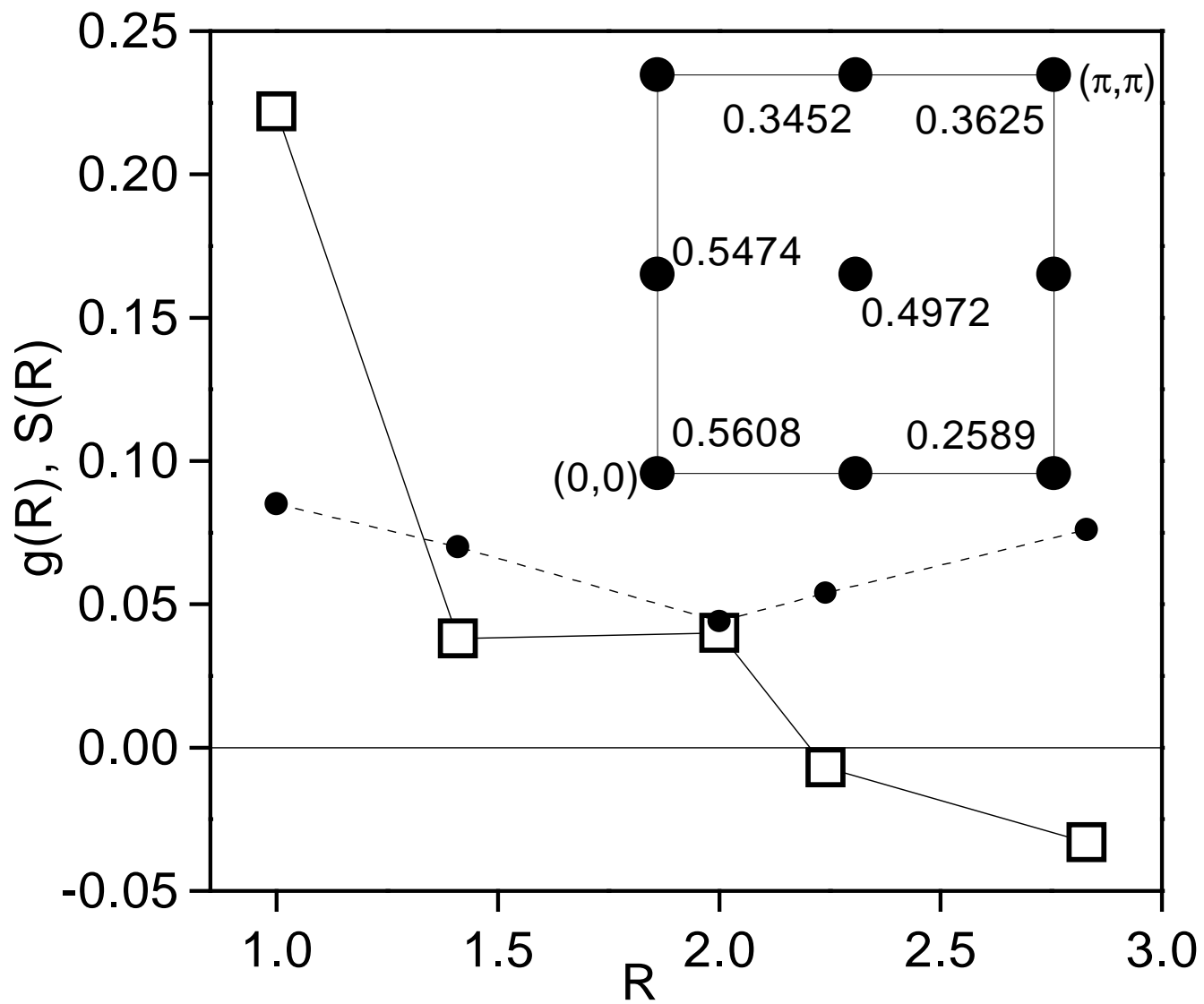


Fig. 11

